

ACCELERATING FIELD MEASUREMENT IN 3GHZ PULSED CAVITIES

G. Bienvenu, J. Le Duff, C. Thomas[#], LAL, BP 34, 91898 ORSAY CEDEX, FRANCE

Abstract

The achievable limiting RF field for S-Band and L-Band superconducting cavities is still an open question today. Previous studies on Sn and In [1] have shown that a surface magnetic field B_s higher than the critical thermodynamic field B_c might be reached. The ultimate limiting field is then the superheating field B_{sh} ($B_{sh} = 240$ mT or $E_{acc} = 60$ MV/m for Nb at $T = 0$ K). However, the maximum accelerating field observed so far is in the range $E_{acc} = 37-40$ MV/m for the best 1.3 GHz Nb cavities. A dedicated facility (NEPAL Supra Test Facility) is currently used at LAL for measuring B_{sh} on bulk Nb 3 GHz cavities supplied by INFN-Genova. High power pulses (4.5 μ s, up to 5 MW) are used to reach B_{sh} before cavity thermal breakdown occurs. A method for analyzing the response of a SRF cavity when subjected to pulsed high RF power pioneered at SLAC [2] was developed and the corresponding numerical simulation results were validated by comparison with experimental data. This technique is successfully applied to detect E_{acc} and E_{rf}^{max} at which the cavity magnetic breakdown occurs. Magnetic penetration depth (λ) measurements were also performed with a low RF level test bed and the corresponding data analyzed and then compared to theoretical predictions.

1 INTRODUCTION

The maximum achieved accelerating fields in SRF cavities are usually limited by field emission and thermal breakdown. These two limits have been pushed back thanks to improvements of niobium purity, cavity preparation, assembling and conditioning techniques. In principle, a theoretical limit of the surface field higher than B_c (i.e $B_c = 200$ mT or 50MV/m accelerating field E_{acc} for TESLA shape bulk niobium (Nb) cavities at $T = 0$ K) is expected in CW mode of operation. Previous RF measurements performed on indium and tin samples and the corresponding theoretical estimation have shown that $B_s > B_c$ might be reached [1]. Moreover, the fundamental limit B_{sh} of bulk Nb is now close to being reached [3]. Due to lack of sufficient experimental data on B_{sh} for Nb, it is important to measure this parameter precisely.

2 PENETRATION DEPTH SUPERHEATING MAGNETIC FIELD

In this section, we briefly summarize the useful relationships dealing with λ and B_{sh} according to different theories.

2.1 Penetration depth

The magnetic penetration depth corresponds to the length of the penetration of a magnetic field in a superconductor. Introduced to explain the Meissner effect, it was first quantified by London as the London penetration depth. Later, Gorter and Casimir introduced the temperature dependence of the super electrons density. The penetration depth is temperature dependent and given by :

$$\lambda(t) = \frac{\lambda_L}{\sqrt{1-t^4}} \quad (1)$$

where t is the reduced temperature ($t = T/T_c$) and T_c the critical temperature. The temperature dependence found by Bardeen, Cooper and Schrieffer [4] agrees with (1) except very close to T_c . Ginzburg and Landau predict a temperature variation of λ different from (1) :

$$\lambda(t) = \frac{\lambda_L}{\sqrt{1-t}} \quad (2)$$

Pippard [5] observed the increase of the penetration depth as the electron mean free path decreased. So the penetration depth depends on the purity of the superconductor. Pippard introduces the concept of coherence length in the London equation leading to a electron mean free path (l_e) dependent penetration depth:

$$\lambda(t) = \lambda_L \sqrt{1 + \frac{1}{\alpha l_e}} \quad (3)$$

where α is a constant determined from experiments ($\alpha = 0.8$). This expression, valid for type II

[#] E-mail: cthomas@lal.in2p3.fr

superconductors in the London limit, becomes, for type I superconductors in the Pippard limit :

$$\lambda_{\infty} = \left(\frac{\sqrt{3}}{2} \xi_0 \lambda_L^2 \right)^{1/3} \quad (4)$$

The expression found by Pippard are also temperature dependant following the Gorter-Casimir model [6].

The Ginzburg Landau model provides two expressions of the penetration depth depending on the limit considered. For clean superconductors :

$$\lambda(t) = \frac{\lambda_L}{(1-t)} \quad (5)$$

For dirty superconductors :

$$\lambda(t) = \frac{\lambda_L}{\sqrt{2}} \sqrt{\frac{\xi_0}{1.33l_e}} \frac{1}{\sqrt{1-t}} \quad (6)$$

As the mean free path decreases, the penetration depth increases.

2.2 Superheating magnetic field

For Type-II superconductors such as niobium, subjected to an external magnetic field B_a (static or slowly varying), the Meissner effect persists up to the first critical field, B_{c1} . For B_a lying between B_{c1} and B_{c2} , normal conducting areas are nucleated : this thermodynamic state is called the mixed state. Beyond B_{c2} , superconductivity is completely destroyed. Moreover, in the case of non-zero B_a , the transition from superconducting to normal conducting state is of first order. In this case, superheating is possible and a magnetic field (B_{sh}) higher than the critical field B_{c1} could then be sustained by the superconducting material. The superheating field B_{sh} is related to the critical thermodynamic field B_c . According to Ginzburg-Landau (GL) theory, we distinguish two kinds of superconductors depending on the value of the material's GL parameter

$\kappa = \frac{\lambda_{GL}}{\xi_{GL}}$ where ξ_{GL} is the GL coherence length :

- For type I superconductors, $B_{sh} = \frac{0.89}{\sqrt{\kappa_{GL}}} B_C$
- For type II, $B_{sh} = 0.75 B_C$

Note that niobium, which is a type II superconductor but with a peculiar behaviour due to its κ value being close to

the critical value $\kappa_{GL}^{Nb} = \frac{1}{\sqrt{2}}$, we have :

$$B_{sh} = 1.2 B_C \quad (7)$$

3 METHOD OF λ MEASUREMENT

The cavity resonant frequency is influenced by the magnetic penetration depth which is a temperature dependent parameter. More precisely, the reactive component of the cavity surface impedance X is related to the resonant frequency, f , by the formula :

$$X = 2G \frac{f - f_0}{f_0} \quad (8)$$

where G is the geometric factor and f_0 is the frequency of an ideal cavity (perfectly conducting). Moreover, X is proportional to the frequency and magnetic penetration depth : $X = 2\pi f \mu_0 \lambda$. Consequently, starting at an initial temperature $T = 4.2$ K and recording the cavity frequency shift due to temperature variation, we can easily deduce the corresponding $\Delta\lambda$:

$$\Delta\lambda(T) = \lambda(T) - \lambda(4.2) = \frac{G}{\pi \mu_0} \frac{\Delta f}{f(4.2)^2} \quad (9)$$

4 RESULTS OF λ MEASUREMENT

4.1 λ measurement on the cavity GEN-1

The cavity GEN-1 was fabricated at Genova by the group of R. Parodi.

The procedure described above was used and the corresponding data are presented in figure (1).

Below 6 K, the electron density decays exponentially so the data were analysed for temperature greater than 6 K (8.5K in our case). The data are fitted to the theoretical relations (Eq.1-2). From the results, no criterion allow us to separate the two theories. They equally fit the datas in the same range of temperature. The slopes and the mean free path have been determined by linear regression from respectively (Eq. 3) and (Eq. 6). The RRR is deduced from $l = 60$ RRR where l is given in Å. Table (1) sums up the results.

Table 1 : Values of the slopes, mean free path and RRR given by the different models

	Gorter-Casimir, Pippard	Ginzburg-Landau
Slope (nm)	29	16
l_e (nm)	381	38
RRR	64	6

These results differ (33%) from previous results obtained by Maxfield [7] and Waldram [8]. They measured the frequency shift with an inductance method on samples.

This has to be accounted on the well known RRR decrease when Niobium sheets are stamped.

The RRR value found by the GL method is far beyond the GC-Pippard one. The explanation comes from the validity interval of the GL theory. Valid close to T_c , GL theory does not work at lower T. The lack of points in this area does not allow us to draw a conclusion.

The fitting parameters are very sensitive to the Nb critical temperature T_c and the London penetration depth λ_L . T_c has been assumed to 9.2 K. But measurements have shown variations between 9.1-9.4 K [9]. To conclude, one has to measure the transition temperature.

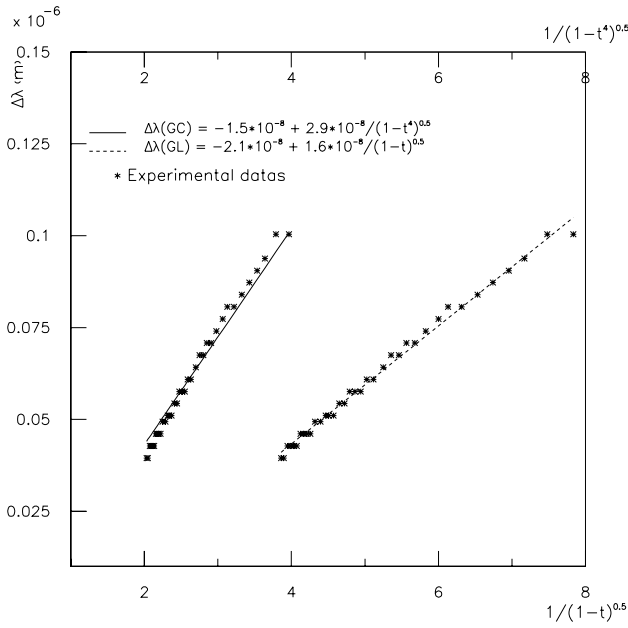


Figure 1 : Relative magnetic penetration depth for cavity GEN1 versus temperature

The estimated RRR obtained from Nb impurities (O, C, N) [10] is 40. The discrepancy between the RRR deduced from λ_{GC} (62) and the estimated (40) one could be explained by RRR decrease near the Nb surface [11].

4.2 λ measurement on the cavity LAL03-C

The cavity LAL03-C was stamped and electron beam welded at LAL. The $\Delta\lambda$ has been measured at IPN and the estimated RRR was 52. The RRR evaluated on a sample which has followed the same chemical and heat treatment by the residual resistivity measurement was 140. The discrepancy between the two RRR's could be explained by RRR decrease when the Nb sheet are stamped.

5 METHOD OF B_{MAX} MEASUREMENT

In most cases, the maximum accelerating field is limited, in DC or long RF pulsed mode (1-10 ms) by cavity thermal breakdown. To circumvent this problem, we use RF pulses of duration $T = 1-4.5 \mu s$ which are much shorter than the characteristic time needed for cavity thermal breakdown or quench induced by anomalous RF losses to occur ($100 \mu s$ [12]). In order to achieve a good transfer efficiency between the RF source and the cavity, a strong external coupling is needed (i.e $Q_{ext} = 5 \cdot 10^4$). As long as the cavity is in the superconducting state

($Q_0(4.2 K) \approx 7 \cdot 10^7$), the cavity decay time $\tau = \frac{Q_L}{\omega}$,

where Q_L is the loaded quality factor, is dominated by the external coupling (i.e $t \approx Q_e/\omega$). When a thermal or magnetic breakdown occurs, Q_0 jumps instantaneously to 10^5 and consequently τ decreases. The emitted power

integral, at the end of the pulse, $U_e = \int A \exp\left(\frac{-t}{\tau}\right) dt$,

which is proportional to the incident power integral U_i , when the cavity is in the superconducting state, shows a deviation from the linear behaviour when the cavity quenches (i.e transition to the normal state) as illustrated in figure (2).

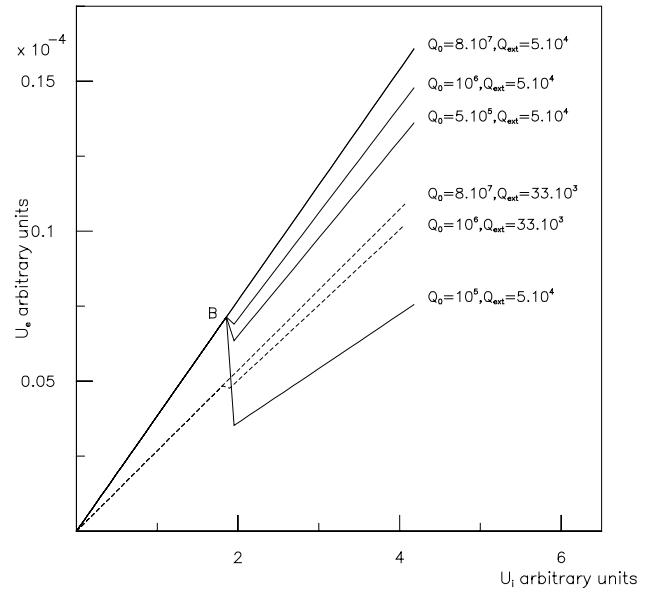


Figure 2 : Simulations of the variation of the emitted power integral versus the incident power integral

The point, where such a deviation (eq. jump of U_e) is initiated and referred to as "B" in this figure, corresponds exactly to the quench field. Note that other methods of quench field measurements are not appropriate to our test stand [13].

6 EXPERIMENTAL APPARATUS AND RESULTS

In order to reach a high accelerating field, we use a 3 GHz-35 MW klystron with a maximum pulse length of 4.5 μ s. Block diagram of the experimental set-up is shown in figure (3). It is close to the one used at SLAC [14]. Data acquisition of all the experimental parameters and processing (RF signal integration) is performed using a dedicated Labview™ program.

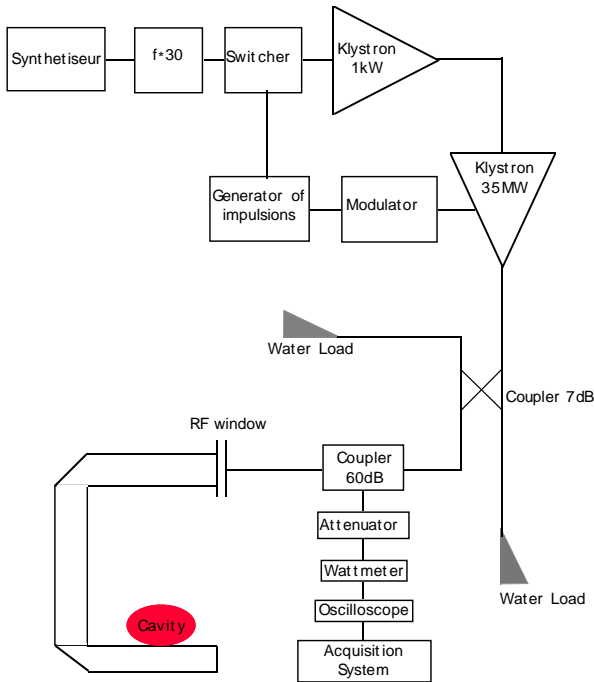


Figure 3 : Schematic of experimental set-up

Experimental runs were performed on two cavities. Results, for cavity CAT2, are displayed in figure (4). The shape of the experimental curve is close to the simulation results (see figure (3)) except for fields lower than 20MV/m. For the corresponding incident power, the klystron is unstable. Therefore, data below 20MV/m are not considered. We clearly observe a linear part of U_e versus U_i up to a critical value of U_i ($U_i^c \approx 1.7$ J). At this value U_e decreases less sharper than expected. The value of the maximum E_{acc} and hence B_s at which the cavity magnetic breakdown occurs is respectively 43.5 MV/m and 141.9 mT. The difference between experimental and theoretical results (11%) is within the measurement errors. The ratio between experimental maximum magnetic field

and critical field is 1.12. The difference from the expected ratio (1.2) is within the experimental error.

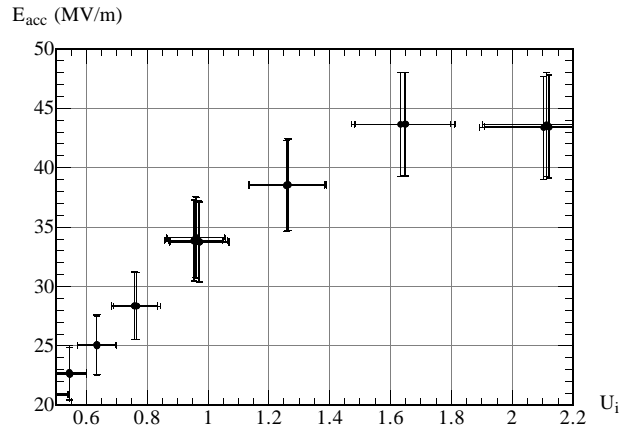


Figure 4 : Accelerating field versus integral of incident power (performed at $T = 4.2$ K on cavity CAT2)

7 ACKNOWLEDGEMENT

We would like to thank J.N.Cayla for his technical support, G.Arnaud, Ph.Dufresne and M.Roch for their assistance concerning vacuum and cryogenics. We would like to thank also the IPN Superconducting cavity group for constructive discussions and allowing us to test their cavity.

8 REFERENCES

- [1] T. Yogi al., Phys. Rev. Let. 39, 826 (1977)
- [2] I. E. Campisi al. , SLAC/AP-16 (1984)
- [3] E. Kako al., Proc. PAC'99, Vol. 1, 432 (1999)
- [4] J. Bardeen, L. N. Cooper and J. R. Schrieffer, Phys. Rev. 108, 1175 (1957)
- [5] A. B. Pippard, Proc. of Roy. Soc. (London), A203, 98 (1950), A. B. Pippard, Proc. of Roy. Soc. (London), A216, 547 (1953)
- [6] J. Daunt al. , Phys. Rev. 74, 842 (1948)
- [7] J. R. Waldram, Adv. Phys. 13, 2 (1964)
- [8] B. W. Maxfield and W. L. MacLean, Phys. Rev. 139, 1515 (1965)
- [9] M. Cyrot and al. , "Introduction of superconductivity and High Tc Materials", p. 113 (1992)
- [10] M. Fouaidy, Private communication
- [11] C. Antoine and al. , Proc. of 8th SRF Workshop, Abano Terme (1997)
- [12] T. Junquera, Adv. Cryo. Eng. , 43
- [13] T. Hays and al. , SRF980804-06, LNS, Cornell University
- [14] I. E. Campisi al. , SLAC/AP-58 (1987)